Unified Stochastic Geometry Analysis of Downlink Cellular Networks

Imène Trigui*, Sofiène Affes†, and Ben Liang*
*University of Toronto 10 King's College Road Toronto, Ontario M5S 3G4, Canada.
†INRS-EMT, 800, de la Gauchetiere Ouest, Bureau 6900, Montreal, H5A 1K6, Qc, Canada

***Abstract*—Statistical characterization of the signal-to-interference-plus-noise ratio (SINR) via its cumulative distribution function (CDF) is ubiquitous in a vast majority of technical contributions in the area of cellular networks since it boils down to averaging the Laplace transform of the aggregate interference, a benefit accorded at the expense of confinement to the simplistic Rayleigh fading. In this work, to capture diverse fading channels that appear in realistic outdoor/indoor wireless communication scenarios, we tackle the problem differently. By exploting the moment generating function (MGF) of the SINR, we succeed in analytically assessing cellular networks performance, namely the achievable rate and and the bit error probability (BEP), over the shadowed κ-μ, κ-μ and η-μ fading models. These models offer higher flexibility to capture diverse and more realistic fading environments than the classical Rayleigh, Nakagami-m, and Rician ones.**

***Index Terms*—Cellular Networks, Fading Channels, Average Rate, Error Probability, LOS, NLOS, Stochastic Geometry, Poisson Point Process.**

I. INTRODUCTION

Cellular networks modeling and analysis is a vibrant topic that keeps taking new dimensions in complexity as to mirror the evolution if not revolution of wireless networks from the first to the upcoming fifth wireless technology generation (5G). As a key enabler to realize 5G wireless networks, heterogeneous networks (HetNets) are indeed the most influential solution that guarantees higher data rates and macrocell traffic offloading, while providing dedicated capacity to homes, enterprises, or urban hot spots. To cope with such evolution, stochastic geometry proved to be a very powerful tool for reproducing large-scale spatial randomness, an intrinsic property of emerging cellular networks, as well as different sources of uncertainties (such as multipath fading, shadowing, and power control) within tractable and accurate mathematical frameworks [1], [3].

In the last decade, many contributions spearheaded this line of research by developing all aspects of the stochastic geometry models(cf. [1]- [6] and references therein), except for the fading environments. As far as the fading model is concerned, the Rayleigh fading has been commonly assumed, with only some proposals incorporating the Nakagami-m fading, yet merely with integer parameter values [7], [8]. Such particular fading distributions, by leading to exponential expressions for the conditional SINR that enable averaging via the MGF of the interference, have very often implied very similar mathematical models in their analysis steps. Strikingly, due to Rayleigh assumption, characterizing the SINR via its cumulative distribution function (CDF) is ubiquitous in almost all pioneering contributions pertaining to cellular networks modeling [1]-[6].

Such infatuation with Rayleigh and Nakagami-m has, however, limited legitimacy according to [9], who argued that these fading models may fail to capture new and more realistic fading environments. Besides ignoring the line-of-sight (LOS) component in the received signal, which is prominent in outdoor cellular communications, the Rayleigh model is a single-parameter fading model that is not flexible enough to accurately represent complex indoor fading environments. The diagnosis for Rayleigh fading is even more pessimistic in future femtocells where multiple LOSs may be created by reflections in close proximity to the BSs and/or users or may appear in millimeter wave (mmW) communications [10]. With Nakagami-m fading, stochastic geometry analysis necessitates for tractability an integer value for m [8], thereby limiting the applicability of the model in setup scenarios that capture practical multipath conditions.

As a step forward to bridge this gap in the literature, this work incorporates versatile multiple-parameter fading models into tractable stochastic geometry analysis. These fading models include the shadowed κ-μ distribution [11], the generalized Rician or the κ-μ distribution, and the η-μ distribution [12]. Besides their elegance, these models are governed by more than two tunable parameters endowing them with high flexibility to capture a broad range of fading channels, whence their practical significance. These fading models offer far better and much more flexible representations of practical fading LOS, NLOS, and shadowed channels than the Rayleigh and Nakagami-m distributions.

Although some works have considered already shadowed κ-μ fading in the context of stochastic geometry (e.g., [13], [14]), they relied on series representation methods (e.g., infinite series in [13] and Laguerre polynomial series in [14]) thereby expressing the interference functionals as an infinite series of higher order derivative

978-1-5386-3531-5/17/$31.00

terms given by the Laplace transform of the interference power. These methods cannot lend themselves to closed-form expressions and hence require complex numerical evaluation.

To the best of the authors' knowledge, this paper is pioneer in introducing a general approach of incorporating the comprehensive shadowed κ-μ, κ-μ and η-μ fading models into an exact and unified stochastic geometry analysis.

II. NETWORK AND CHANNEL MODELS

We consider a downlink single-tier cellular network where single-antennas BSs are deployed according to a homogeneous PPP Ψ with intensity λ and a typical single-antenna mobile user is located at the origin. It is assumed that all the BSs have the same transmit power P. Without loss of generality, all BSs are assumed to have an open access policy, and hence, all users can associate with all BSs. The users are assumed to associate to the BSs according to their average radio signal strength (RSS) rule. Similar to [1, Sec. VI], universal frequency reuse is considered with no intra-cell interference.

Further, we adopt the standard path-loss propagation model of power attenuation $r^{-\alpha}$ with the propagation distance r, where $\alpha > 2$ is the path-loss exponent. For simplicity, we assumes that all BSs experience the same path-loss exponent α. Besides we assume that the channel gains between any two generic locations, denoted by h, include all random channel effects such as fading and shadowing. Additionally, we assume the latter to be independent of each other, independent of the spatial locations, symmetric, and identically distributed.

A. Channel Model Distributions

1) The shadowed κ-μ distribution: The shadowed κ-μ distribution is used to account for small scale fading which originates due to LOS or NLOS conditions, whence its extreme versatility including as special cases nearly all linear fading models adopted in the open literature [11, Table I]. In this model, the dominant signal components (DSCs) are subject to Nakagami-m shadowing. The probability density function (PDF) of $h \sim S_{\kappa,\mu,m}(\Omega;\kappa,\mu,m)$ is

$$f_{h,S\kappa-\mu}(y) = \frac{\mu^{\mu} m^{m} (1+\kappa)^{\mu}}{\Gamma(\mu)\Omega^{\mu}(\mu\kappa+m)^{m}} \left(\frac{y}{\Omega}\right)^{\mu-1} e^{-\frac{\mu(1+\kappa)}{\Omega}y} {}_1\mathrm{F}_1\left(m,\nu,\frac{\mu^2\kappa(1+\kappa)}{\Omega(\mu\kappa+m)}y\right), \quad (1)$$

where $\Omega = \mathcal{E}[h]$, κ, μ, and m, are positive real shape parameters, and ${}_1\mathrm{F}_1(\cdot)$ denotes the confluent hypergeometric function of [15, Eq. (13.1.2)]

2) The κ-μ distribution: The κ-μ distribution captures the small-scale variations of the fading signal under LOS conditions [12] and arises form the shadowed κ-μ distribution by eliminating the shadowing of each dominant component when $m \longrightarrow \infty$. The PDF of $h \sim S_{\kappa,\mu}(\Omega;\kappa,\mu)$ is

$$f_{h,\kappa-\mu}(y) = \frac{\mu(1+\kappa)^{\frac{\mu+1}{2}}}{e^{\kappa\mu}\Omega\kappa^{\frac{\mu-1}{2}}} \left(\frac{y}{\Omega}\right)^{\frac{\mu-1}{2}} e^{-\frac{\mu(1+\kappa)}{\Omega}y} \mathrm{I}_{\mu-1}\left(2\mu\sqrt{\frac{\kappa(1+\kappa)}{\Omega}y}\right), \quad (2)$$

where $\Omega = \mathcal{E}[h]$, κ, μ are positive real shape parameters, and $\mathrm{I}_b(\cdot)$ denotes the modified Bessel function of the first kind of order b [15, Eq. 8.431.1].

3) The η-μ distribution: The η-μ distribution represents the small-scale variation of the fading signal in a NLOS condition [12]. The PDF of $h \sim S_{\eta,\mu}(\Omega;\eta,\mu)$ is given by

$$f_{h,\eta-\mu}(y) = \frac{\sqrt{\pi}(1+\eta)^{\mu+\frac{1}{2}}\mu^{\mu+\frac{1}{2}}}{\Gamma(\mu)\Omega\sqrt{\eta}(1-\eta)^{\mu-\frac{1}{2}}} \left(\frac{y}{\Omega}\right)^{\mu-\frac{1}{2}} e^{-\frac{\mu(1+\eta)^2}{2\eta\Omega}y} \mathrm{I}_{\mu-\frac{1}{2}}\left(\frac{\mu(1-\eta)^2}{2\eta\Omega}y\right). \quad (3)$$

where $\Omega = \mathcal{E}[h]$ and η, μ are non-negative real shape parameters.

B. Modeling Methodology

The instantaneous SINR for the tagged user placed at the originand located at a random distance r from its serving BS can be expressed as

$$\mathrm{SINR} = \frac{Phr^{-\alpha}}{\sigma^2 + P\sum_{i\in\Psi^{(\setminus 0)}} h_i r_i^{-\alpha}} = \frac{hr^{-\alpha}}{\frac{\sigma^2}{P} + \mathcal{I}}, \quad (4)$$

where σ^2 is the noise power, $\Phi^{(\setminus 0)}$ is the point process representing the interfering BSs (excluding the serving BS) on the tagged channel, and the random variable $\mathcal{I} = \sum_{i\in\Psi^{(\setminus 0)}} h_i r_i^{-\alpha}$ denotes the aggregate interference at the tagged user from $\Psi^{(\setminus 0)}$. Note that in stochastic geometry analysis, spatial average performance metrics requires the pdf of r, which is given in a PPP network with RSS association as $f_r(x) = 2\pi\lambda x e^{-\pi\lambda x^2}, \quad r \geq 0$ [1].

Lemma 1: The MGF of the SINR can be calculated as

$$M_{\mathrm{SINR}}(s) = 1 - 2\sqrt{s}\int_0^{\infty} \underbrace{\mathcal{E}_h\left[\sqrt{h}\mathrm{J}_1\left(2\sqrt{sh}\xi\right)\right]}_{\Sigma} \mathcal{E}_r\left[\exp\left(-\frac{\sigma^2}{P}\xi^2 r^{\alpha}\right)\mathcal{L}_{\mathcal{I}}(\xi^2 r^{\alpha})\right] d\xi, \quad (5)$$

where $\mathcal{E}_x[.]$ is the expectation with respect to the random variable x, $\mathrm{J}_1(\cdot)$ is the Bessel function of the second kind and first order [15, Eq. 8.402], and $\mathcal{L}_{\mathcal{I}}(s) = \mathcal{E}\left[e^{-sI}\right]$ denotes the Laplace transform of the aggregate interference.

Proof: Given the $\mathrm{SINR} = \frac{hr^{-\alpha}}{\frac{\sigma^2}{P}+\mathcal{I}(r)}$, its MGF, defined as $M_{\mathrm{SINR}}(s) \triangleq \mathcal{E}_{r,h,\mathcal{I}}\left[\exp\left(-s\mathrm{SINR}\right)\right]$, is evaluated as

$$M_{\text{SINR}}(s) = \mathcal{E}_{r,h}\left[\int_0^\infty \exp\left(-\frac{shr^{-\alpha}}{y}\right) f_{\mathcal{I}+\frac{\sigma^2}{P}}(y)dy\right]$$
$$= \mathcal{E}_{r,h}\left[\mathcal{L}_{\frac{1}{I+\frac{\sigma^2}{P}}}\left(shr^{-\alpha}\right)\right]$$
$$\overset{(a)}{=} 1-2\mathcal{E}_r\left[\sqrt{sr^{-\alpha}}\int_0^\infty \mathcal{E}_h\left[\sqrt{h}\mathrm{J}_1\left(2\sqrt{shr^{-\alpha}\xi}\right)\right]\mathcal{L}_{\mathcal{I}+\frac{\sigma^2}{P}}(\xi^2)d\xi\right], \quad (6)$$

where (a) follows from applying [16, Theoerm 1]. Then Lemma 1 is obtained by a change of variable relabeling $\xi r^{-\frac{\alpha}{2}}$ as ξ, while taking into account the linearity and the time shifting properties of the Laplace transform implying that $\mathcal{L}_{\mathcal{I}+\frac{\sigma^2}{P}}(x) = e^{-\frac{\sigma^2}{P}x}\mathcal{L}_{\mathcal{I}}(x)$.

It is worth emphasizing that Σ in (5) is independent of the variable $\mathcal{L}_{\mathcal{I}}$ and is a function of the fading parameters only. Hence, for known fading parameters, Σ is a constant w.r.t. the interference Laplace transform. This key property of Lemma 1 makes the latter a powerful baseline model to build upon in terms of developing tractable analytical models for cellular network, namely by extending the results of this paper to many other directions. Without any hope of discussing them all, the most prominent directions include uplink and multi-tier downlink performance analysis. Although extended in numerous ways to date [1]-[6], these three models (i.e., downlink, uplink and multi-tier) have never been considered from the standpoint of (5). Interestingly, Lemma 1 not only promote general and generic fading channels but also other generalization aspects such as the the effect of LOS/NLOS propagation where the probability with which a BS is NLOS (also termed blocking probability) is dependent on the distance between the BS and the receiver of interest [18].

Hereafter, by applying (5), we characterize the SINR by deriving for the first time its MGF in generalized fading channels.

III. UNIFIED ANALYSIS OF THE SINR STATISTICS

We now state our main and most general results from which all other results in the subsequent sections shall follow.

Theorem 1: The MGF of the SINR over shadowed κ-μ fading is

$$M^{S\kappa\mu}_{\text{SINR}}(s) = 1-\frac{\Omega s}{\left(\frac{\mu\kappa}{m}+1\right)^m(1+\kappa)}\int_0^\infty \Psi_1\left(\mu+1, m; 2, \mu; \right.$$
$$\left.\frac{-s\xi\Omega}{\mu(1+\kappa)}, \frac{\mu\kappa}{\mu\kappa+m}\right)\mathcal{E}_r\left[\exp\left(-\xi r^\alpha\frac{\sigma^2}{P}\right)\mathcal{L}_I^{S\kappa\mu}(\xi r^\alpha)\right]d\xi, \quad (7)$$

where $\Psi_1(\cdot,\cdot;\cdot,\cdot;\cdot,\cdot)$ denotes the Humbert function of the first kind [19, Eq. 1.2]. The Laplace transform of the aggregate interference when the receiver interfering link suffers from arbitrary shadowed κ-μ fading, i.e., $h_{i\in\Phi(\backslash 0)} \sim S_{\kappa,\mu,m}(\Omega_I;\kappa_I,\mu_I,m_I)$, is denoted as $\mathcal{L}_I^{S\kappa\mu}$ and obtained, when $\mu_I \leq m_I$, as in (8) and becomes (9) when $\mu_I \geq m_I$, where $\Theta = \frac{\Omega_I}{\mu_I(1+\kappa_I)}$, $\Xi = \frac{(\mu_I\kappa+m_I)\Omega_I}{m_I\mu_I(1+\kappa_I)}$. Moreover, ${}_2\mathrm{F}_1(a,b,c,x)$ and $\mathrm{F}_1(a,b,b';c;x,y)$ denote the Gauss hypergeometric function [15, Eq. 9.100] and the first Appell's hypergeometric function [15, Eq. 9.180.1], respectively, and $\binom{a}{b} = \Gamma(a)\Gamma(b)/\Gamma(a+b)$ is the binomial coefficient.

Proof: [17, Appendix B].

Theorem 2: The MGF of the SINR over κ-μ fading is

$$M^{\kappa\mu}_{\text{SINR}}(s) = 1-\frac{\Omega e^{-\kappa\mu}s}{(1+\kappa)}\int_0^\infty \Psi_2\left(\mu+1; 2, \mu; \frac{-s\xi\Omega}{\mu(1+\kappa)}, \mu\kappa\right)$$
$$\mathcal{E}_r\left[\exp\left(-\xi r^\alpha\frac{\sigma^2}{P}\right)\mathcal{L}_I^{\kappa\mu}(\xi r^\alpha)\right]d\xi, \quad (10)$$

where $\Psi_2(\cdot,\cdot;\cdot,\cdot;\cdot,\cdot)$ denotes the Humbert function of the second kind [19, Eq. 1.3], and $\mathcal{L}_I^{\kappa\mu}$ denotes the Laplace transform of the aggregate interference under κ-μ fading, i.e., $h_{i\in\Phi(\backslash 0)} \sim S_{\kappa,\mu}(\Omega_I;\kappa_I,\mu_I)$. Furthermore, $\mathcal{L}_I^{\kappa\mu}$ is obtained as in (11).

Proof: [17, Appendix C].

Theorem 3: The MGF of the SINR over η-μ fading is

$$M^{\eta\mu}_{\text{SINR}}(s) = 1-\frac{2\Omega\eta^{\mu+1}s}{\eta+1}\int_0^\infty \Psi_1\left(2\mu+1, \mu; 2, 2\mu; \right.$$
$$\left.\frac{-s\xi\Omega\eta}{\mu(1+\eta)}, 1-\eta\right)\mathcal{E}_r\left[\exp\left(-\xi r^\alpha\frac{\sigma^2}{P}\right)\mathcal{L}_I^{\eta\mu}(\xi r^\alpha)\right]d\xi, \quad (12)$$

where the Laplace transform of the aggregate interference $h_{i\in\Phi(\backslash 0)} \sim S_{\eta,\mu}(\Omega_I;\eta_I,\mu_I)$, denoted as $\mathcal{L}_I^{\eta\mu} = \mathcal{L}_I^{S\kappa\mu}(\underline{m}_I \leftarrow \mu_I, \underline{\mu}_I \leftarrow 2\mu_I, \underline{\kappa}_I \leftarrow \frac{1-\eta_I}{2\eta_I})$, with $\mathcal{L}_I^{S\kappa\mu}$ given in (9).

Proof: From (1), when $m = \mu/2$, we resort to the reduction formula of ${}_1\mathrm{F}_1(\cdot)$ given by [15, Eq. 9.6.47]

$${}_1\mathrm{F}_1(\beta, 2\beta, z) = 2^{2\beta-1}\Gamma\left(\beta+\frac{1}{2}\right)z^{\frac{1}{2}-\beta}e^{z/2}\mathrm{I}_{\beta-\frac{1}{2}}\left(\frac{z}{2}\right), \quad (13)$$

readily yielding (3) after some algebraic manipulations. Since $m_I = \mu_I/2 \leq \mu_I$, then $\mathcal{L}_I^{\kappa\mu}$ reduces from $\mathcal{L}_I^{S\kappa\mu}$ in (9) by setting $\underline{m}_I = \mu_I$, $\underline{\mu}_I = 2\mu_I$, and $\underline{\kappa}_I = \frac{1-\eta_I}{2\eta_I}$.

Theorem 4: The MGF of the SINR over arbitrary Nakagami-m fading is given by

$$M^m_{\text{SINR}}(s) = 1-\Omega s\int_0^\infty {}_1\mathrm{F}_1\left(m+1, 2; \frac{-s\Omega\xi}{m}\right)$$
$$\mathcal{E}_r\left[\exp\left(-\frac{\xi r^\alpha\sigma^2}{P}\right)\mathcal{L}_I^m(\xi r^\alpha)\right]d\xi, \quad (14)$$

and the Laplace transform of the aggregate interference under Nakagami-m fading $\mathcal{L}_I^m$ is given by

$$\mathcal{L}_I^m(\xi r^\alpha) = e^{-\pi\lambda r^2\left({}_2\mathrm{F}_1\left(-\frac{2}{\alpha}, m_I, 1-\frac{2}{\alpha}; -\frac{\Omega_I}{m_I}\xi\right)-1\right)}. \quad (15)$$

Proof: The Nakagami-m fading distribution arises as a particular case of the more general shadowed κ-μ model when $m = \mu$. However, this simplification is not straightforward and actually requires further manipulations shown in details in [17, Appendix D].

It is worthwhile to note that $\mathcal{L}_I^m$ in (15) is a well-known result in the area of cellular networks analysis

$$\mathcal{L}_I^{S\kappa\mu}(\xi r^\alpha) = \exp\Bigg(- \pi\lambda r^2 \Bigg(\sum_{k=1}^{m_I} \frac{\binom{k}{m_I}\Xi^k\xi^k}{\frac{\alpha k}{2}-1} {}_2\mathrm{F}_1\left(m_I, k-\frac{2}{\alpha}, k+1-\frac{2}{\alpha}, -\Xi\xi\right) - \sum_{n=1}^{m_I-\mu_I} \frac{\binom{n}{m_I-\mu_I}\Theta^n\xi^n}{\frac{\alpha n}{2}-1} {}_2\mathrm{F}_1\left(m_I, n-\frac{2}{\alpha}, n+1-\frac{2}{\alpha}, -\Xi\xi\right)\Bigg)\Bigg), \tag{8}$$

$$\mathcal{L}_I^{S\kappa\mu}(\xi r^\alpha) = \exp\Bigg(- \pi\lambda r^2 \sum_{n,k;(n,k)\neq(0,0)}^{m_I,\mu_I-m_I} \frac{\binom{\mu_I-m_I}{k}\binom{m_I}{n}\Theta^k\Xi^n\xi^{k+n}}{\frac{\alpha(n+k)}{2}-1} \mathrm{F}_1\left(n+k-\frac{2}{\alpha}, \mu_I-m_I, m_I, n+k+1-\frac{2}{\alpha}, -\Theta\xi, -\Xi\xi\right)\Bigg), \tag{9}$$

$$\mathcal{L}_I^{\kappa\mu}(\xi r^\alpha) = \exp\Bigg(- \pi\lambda r^2 \frac{\mu(1+\kappa_I)^{\mu_I}}{e^{\kappa_I\mu_I}\Omega_I^{\mu_I}} \sum_{k=0}^{\infty} \frac{\left(\frac{\mu_I^2\kappa_I(1+\kappa_I)}{\Omega_I}\right)^k}{k!} \sum_{n=1}^{\mu_I+k} \frac{\binom{\mu_I+k}{n}\left(\frac{\xi\Omega_I}{\mu_I\kappa_I(1+\kappa_I)}\right)^n}{\frac{\alpha n}{2}-1} {}_2\mathrm{F}_1\left(\mu_I+k-2, n-\frac{2}{\alpha}, n+1-\frac{2}{\alpha}, -\frac{\xi\Omega_I}{\mu_I\kappa_I(1+\kappa_I)}\right)\Bigg). \tag{11}$$

over Nakagami-m fading [8]. While $\mathcal{L}_I^m$ has so far been presented as a fundamental finding in previous works, it becomes in this contribution a secondary result that simply reduces from a more general performance analysis framework.

The MGF of the SINR for Rayleigh fading, extensively adopted in the literature [1]-[6], reduces simply from (14) when $m = m_I = 1$.

While applying the shadowed κ-μ or the κ-μ (to capture different DSCs scenarios) to the tagged user link is quite intuitive (typically in the case of future femtocells and picocells), it might not be as much obvious to do so to the interference links. Actually, in a typical urban deployment, interfering channels are less likely to experience LOS than the direct link. However, destructive LOS interference may also happen in practice, namely in suburban and rural areas having wide parks and open spaces. In this work, the treatment of the tagged user link is independent from its interference counterpart as can be seen from (5). This dissociation is very appreciable since it allows modeling cellular networks with direct and interfering links experiencing asymmetric fading (i.e., different fading models). Although not shown explicitly in this work, cellular networks performance under asymmetric fading can be easily assessed by swapping $\mathcal{L}_I$ in (8), (9), (11), and (15).

The new fundamental statistics disclosed in Theorems 1 to 4 provide a novel unifying analysis framework for of a variety of extremely important fading distributions. In some particular cases, the obtained formulas reduce to previously well-known major results in the literature. Besides, even though this work focuses on the shadowed κ-μ, κ-μ, and η-μ distributions, our new analysis framework is extensible to any other faidng/shadowing distribution as long as the quantity pertaining to the expectation over h in (5) (i.e., Σ) can be obtained in closed form.

IV. AVERAGE ACHIEVABLE RATE

The average transmission rate $C \triangleq \mathcal{E}[\ln(1+\text{SINR})]$, as defined by Shannon's capacity, is evaluated using the MGF transform in [20, Lemma 21] as

$$C = \int_0^\infty \frac{\exp\{-s\}}{s}\left(1 - M_{\text{SINR}}(s)\right) ds. \tag{16}$$

The average rate is computed in nats/Hz (1 bit $= \ln(2) = 0.6934$ nats) for a typical user assumed to achieve the Shannon bound at its instantaneous SINR. We state now the main theorems that give the ergodic capacity of a typical mobile user on the downlink.

Theorem 5: The average ergodic rate of a typical mobile user on the downlink over shadowed κ-μ fading is

$$C^{S\kappa\mu}(\lambda,\alpha) = \frac{\Omega}{\left(\frac{\mu\kappa}{m}+1\right)^m(1+\kappa)} \int_0^\infty \mathrm{F}_2\Bigg(\mu+1, m, 1; 2, \mu; \frac{\mu\kappa}{\mu\kappa+m}, \frac{-\xi\Omega}{\mu(1+\kappa)}\Bigg) \mathcal{E}_r\left[\exp\left(-\xi r^\alpha \frac{\sigma^2}{P}\right)\mathcal{L}_I^{S\kappa\mu}(\xi r^\alpha)\right] d\xi, \tag{17}$$

where $\mathrm{F}_2(a,b,b';c,c';x,y)$ stands for the Appell's hypergeometric function of the second kind [15, Eq. 9.180.2], and $\mathcal{L}_I^{\kappa\mu}(\xi r^\alpha)$ is given in (8)-(9).

Proof: Plugging (7) into (16), and resorting to [19]

$$\mathrm{F}_2(a,b,b';c,c';x,y) = \frac{1}{\Gamma(b')}\int_0^\infty t^{b'-1}e^{-t} \Psi_1(a,b;c,c';x,yt)\, dt, \tag{18}$$

yield the desired result after some manipulations.

Theorem 6: The average rate of a typical mobile user at a distance r from its serving BS over κ-μ fading is

$$C^{\kappa\mu}(\lambda,\alpha)=\frac{\Omega e^{-\kappa\mu}}{(1+\kappa)}\int_0^{\infty}\Psi_1\left(\mu+1,1;2,\mu;\mu\kappa,\frac{-\xi\Omega}{\mu(1+\kappa)}\right)\mathcal{E}_r\left[\exp\left(-\xi r^{\alpha}\frac{\sigma^2}{P}\right)\mathcal{L}_I^{\kappa\mu}\left(\xi r^{\alpha}\right)\right]d\xi, \quad (19)$$

where $\mathcal{L}_I^{\kappa\mu}\left(\xi r^{\alpha}\right)$ is given in (11).

Proof: The results follows after substituting (10) into (16) and applying

$$\Psi_1\left(a,b;c,c';x,y\right)=\frac{1}{\Gamma(b)}\int_0^{\infty}t^{b-1}e^{-t}\Psi_2(a,c,c';x,yt)\,dt. \quad (20)$$

Another rationale to get (19) starts from (17) and employs the following limit relation [19]:

$$\lim_{\epsilon\to 0}\mathrm{F}_2\left(\alpha,\frac{b'}{\epsilon},b,c',c;\epsilon x,y\right)=\Psi_1\left(\alpha,b;c',c;b'x,y\right). \quad (21)$$

Corollary 1 (Rice fading): An interesting case to be addressed here is the typical Rice model, which arises from the κ-μ fading when $\mu=1$ and $\kappa=K$ where K is the Rice factor. The ergodic rate under Rice fading is obtained from (19) as

$$C^{Rice}(\lambda,\alpha)=\frac{\Omega e^{-K}}{1+K}\int_0^{\infty}\Psi_1\left(2,1;2,1;K,\frac{-\xi\Omega}{1+K}\right)\mathcal{E}_r\left[\exp\left(-\xi r^{\alpha}\frac{\sigma^2}{P}\right)\mathcal{L}_I^{Rice}\left(\xi r^{\alpha}\right)\right]d\xi, \quad (22)$$

where $\mathcal{L}_I^{Rice}(\xi r^{\alpha})=\mathcal{L}_I^{\kappa\mu}(\xi r^{\alpha},\kappa\leftarrow K,\mu\leftarrow 1)$.

Theorem 7: The average rate of a typical mobile user at a distance r from its serving BS over η-μ fading is

$$C^{\eta\mu}(\lambda,\alpha)=\frac{2\Omega\eta^{\mu+1}}{\eta+1}\int_0^{\infty}\mathrm{F}_2\left(2\mu+1,\mu,1;2,\mu;\frac{-\xi\Omega\eta}{\mu(1+\eta)},1-\eta\right)\mathcal{E}_r\left[\exp\left(-\xi r^{\alpha}\frac{\sigma^2}{P}\right)\mathcal{L}_I^{\eta\mu}\left(\xi r^{\alpha}\right)\right]d\xi. \quad (23)$$

Proof: The result is obtained along the same lines of (17) by performing similar substitutions as in (12).

Theorem 8: The average ergodic rate of a typical mobile user over Nakagami-m fading is

$$C^{m}(\lambda,\alpha)=\int_0^{\infty}\frac{\left(1-\left(1+\frac{\Omega\xi}{m}\right)^{-m}\right)\mathcal{E}_r\left[e^{-\frac{\xi r^{\alpha}\sigma^2}{P}}\mathcal{L}_I^{m}\left(\xi r^{\alpha}\right)\right]}{\xi}d\xi, \quad (24)$$

where $\mathcal{L}_I^{m}\left(\xi r^{\alpha}\right)$ is given in (15).

Proof: The result is a special case of (17) when $m=\mu$. In this case, a reduction formula of the Appell's F_2 function is given in [17, Appendix E]. Alternatively, one can obtain (24) after plugging (14) into (16) and resorting to [15, Eq. 7621.5].

The Rayleigh case reduces from (24) when $m=m_I=1$; a key result previously obtained in [1, Theorem 3], under, however, a more involved expression that encompasses a two-fold integration.

V. AVERAGE BEP UNDER GAUSSIAN SIGNALING APPROXIMATION

This section delves into fine wireless communication details trough BEP analysis by exploiting the Gaussian signaling approximation [6],[8]. Without loss of generality, we focus on the BEP, denoted by $\mathcal{B}$, for coherent M-PSK (phase shift keying) and M-QAM (quadrature amplitude modulation) constellations given by [21]

$$\mathcal{B}=\beta_M\sum_{p=1}^{\tau_M}\mathcal{E}\left[\mathrm{Q}\left(a_p\sqrt{\mathrm{SINR}}\right)\right], \quad (25)$$

where $\mathrm{Q}(\cdot)$ is the Gaussian Q-function and β_M, a_p, and τ_M are modulation-dependent parameters specified in [21].

Hereafter, we provide the BEP performance of a typical mobile user on the downlink under the considered channel models, namely shadowed κ-μ, κ-μ, η-μ, and all other related distributions.

Theorem 8: The average BEP of a cellular downlink over shadowed κ-μ fading is

$$\mathcal{B}^{S\kappa\mu}(\lambda,\alpha)=\frac{\beta_M\tau_M}{2}-\frac{\beta_M\Gamma(\mu+\frac{1}{2})\sqrt{\frac{\Omega}{\mu(1+\kappa)}}}{\sqrt{2}\pi\Gamma(\mu)\left(\frac{\mu\kappa}{m}+1\right)^{m}}\sum_{p=1}^{\tau_M}a_p\int_0^{\infty}\frac{\Psi_1\left(\mu+\frac{1}{2},m;\frac{3}{2},\mu;\frac{-a_p^2\xi\Omega}{2\mu(1+\kappa)},\frac{\mu\kappa}{\mu\kappa+m}\right)}{\sqrt{\xi}}\mathcal{E}_r\left[\exp\left(-\xi r^{\alpha}\frac{\sigma^2}{P}\right)\mathcal{L}_I^{S\kappa\mu}\left(\xi r^{\alpha}\right)\right]d\xi. \quad (26)$$

Proof: Please refer to [17, Appendix F].

Theorem 9: The average BEP of a cellular downlink over κ-μ fading is

$$\mathcal{B}^{\kappa\mu}(\lambda,\alpha)=\frac{\beta_M\tau_M}{2}-\frac{\beta_M\Gamma(\mu+\frac{1}{2})e^{\kappa\mu}\sqrt{\frac{\Omega}{\mu(1+\kappa)}}}{\sqrt{2}\pi\Gamma(\mu)}\sum_{p=1}^{\tau_M}a_p\int_0^{\infty}\frac{\Psi_2\left(\mu+\frac{1}{2};\frac{3}{2},\mu;\frac{-a_p^2\Omega\xi}{2\mu(1+\kappa)},\mu\kappa\right)}{\sqrt{\xi}}\mathcal{E}_r\left[\exp\left(-\xi r^{\alpha}\frac{\sigma^2}{P}\right)\mathcal{L}_I^{\kappa\mu}\left(\xi r^{\alpha}\right)\right]d\xi. \quad (27)$$

Proof: The result follows after recognizing that $\mathcal{B}^{\kappa\mu}(\lambda,\alpha)=\lim_{m\to\infty}\mathcal{B}^{S\kappa\mu}(\lambda,\alpha)$. Then, recalling $\lim_{\epsilon\to 0}\Psi_1\left(a,\frac{b}{\epsilon};c,c';\epsilon w,z\right)=\Psi_2\left(a;c,c';bw,z\right)$, yields the desired result after some manipulations. Note that the same result could be obtained by following similar steps leading to (27) with one difference of using the integral representation of Ψ_2 in [19, Eq. 40]. Notice when $\mu=1$ and $\kappa=K$ that (27) reduces to the BEP expression under Rice fading.

Theorem 10: The average BEP of a cellular downlink over η-μ fading is

$$\mathcal{B}^{\eta\mu}(\lambda,\alpha)=\frac{\beta_M\tau_M}{2}-\frac{\beta_M\eta^{\mu}\Gamma(2\mu+\frac{1}{2})\sqrt{\frac{\Omega\eta}{\mu}}}{\sqrt{2}\pi\Gamma(2\mu)}$$
$$\sum_{p=1}^{\tau_M}a_p\int_0^{\infty}\frac{\Psi_1\left(2\mu+\frac{1}{2},\mu;\frac{3}{2},2\mu;\frac{-a_p^2\xi\Omega\eta}{2\mu(1+\eta)},1-\eta\right)}{\sqrt{\xi}}$$
$$\mathcal{E}_r\left[\exp\left(-\xi r^{\alpha}\frac{\sigma^2}{P}\right)\mathcal{L}_I^{\eta\mu}\left(\xi r^{\alpha}\right)\right]d\xi. \quad (28)$$

Proof: The average BEP over η-μ fading is obtained form (26) by setting $\underline{m}=\mu$, $\underline{\mu}=2\mu$, and $\underline{\kappa}=\frac{1-\eta}{2\eta}$ in both the desired and interfering fading channels and performing the necessary simplifications.

Corollary 5: The average BEP for the downlink cellular communication links in general Nakagami-m fading is

$$\mathcal{B}^{m}(\lambda,\alpha) = \frac{\beta_M\tau_M}{2}-\frac{\beta_M\Gamma(m+\frac{1}{2})\sqrt{\frac{\Omega}{m}}}{\sqrt{2}\pi\Gamma(m)}\sum_{p=1}^{\tau_M}a_p$$
$$\int_0^{\infty}\frac{{}_1\mathrm{F}_1\left(m+\frac{1}{2},\frac{3}{2};\frac{-a_p^2\xi\Omega}{2m}\right)}{\sqrt{\xi}}\mathcal{E}_r\Big[e^{-\xi r^{\alpha}\frac{\sigma^2}{P}}\mathcal{L}_I^{m}\left(\xi r^{\alpha}\right)\Big]d\xi. \quad (29)$$

Proof: The result follows from (26) by setting $m=\mu$ and using the Humbert Ψ_1 function reduction formulas given in [17, Appendix D]. Alternatively, plugging (14) into (25) and resorting to [17, Eq. 76] yield the desired result.

Recently, the authors of [8] investigated the impact of Gaussian signalling under Nakagami-m and derived the corresponding error rates. Although the number of integrals in the obtained BEP expression in (29) is not reduced when compared to [8], our approach discards the necessity for integer m, an assumption made in [8] for the sake of tractability. In practical scenarios, however, the m parameter often takes non-integer values, as argued by [22]. Once again, the significance of this work is highlighted by its very wide scope.

VI. NUMERICAL AND SIMULATION RESULTS

In this section, numerical examples are shown to substantiate the accuracy of the new unified mathematical framework and to confirm its potential for analyzing cellular networks. The simulation setup is summarized in the caption of each figure.

Fig. 1 compares the average rate and average BEP for the κ-μ shadowed fading across a wide range of channel parameters (m, κ, μ). In Fig. 1 (a), $C^{S\kappa\mu}$ is represented as a function of the LOS component in the received wave clusters κ for different values of the μ parameter. We note that a rich scattering (large μ) achieves a higher rate with diminishing returns as κ increases, since increasing μ in the strong LOS scenario has little effect as the performance is dominated by the LOS component. When $m=\mu$, the κ-μ shadowed fading distribution boils down to the Nakagami-m distribution, whence the average rate's independency of κ.

The impact of shadowed LOS components on performance can be observed in Fig. 1 (b), where the average rate under κ-μ shadowed fading is presented as a function of the average SNR for different values of m and considering, respectively, small ($\kappa=1$) and large ($\kappa=20$) LOS components. It can be observed that performance improves with small LOS components ($\kappa=1$) if the latter are affected by heavy shadowing (small m). However, when the shadowing is mild, large LOS components ($\kappa=20$) always improve the average rate. In fact, small m indicates highly fluctuating dominant components, which decrease both the received signal and the aggregate interference powers thereby increasing the SINR level and ultimately achieving higher rates. Conversely, when m is large, the shadowing on the dominant components subsides and κ-μ shadowed fading reduces to κ-μ fading. Moreover, light shadowing always yields higher interference power thereby deteriorating the received SINR level as well as the average rate. Fig. 1 (b) also compares the average rate for various BS densities λ. It can be seen that the average rate of a sparse network ($\lambda\leq 10^{-4}$) is much lower than that of a dense network ($\lambda\geq 10^{-2}$). For example the average average rate is about 0.02 for $\lambda=10^{-4}$ and 1 for $\lambda=10^{-2}$ with $m=0.5$, $\kappa=20$ and SNR $=15$ dB.

Fig. 2 compares the average rate under κ-μ fading versus the BS density λ for different values of the μ parameter. As conjectured in Corollay 1, the network performance is invariant of the network density in an interference-limited condition (large BS intensity). The results show that the rate saturation may happen at certain network density required to obtain sufficiently larger interference power than the noise. In fact, at high SNR, the saturation regime is reached at $\lambda=10^{-2}$, compared to $\lambda\geq 10^{-1}$ in the low SNR regime. In practice, installing more BSs is beneficial to the user performance up to a density point, after which further densification turns out to be extremely ineffective due to faster growth of interference compared to useful signal. This highlights the cardinal importance of interference mitigation, coordination among neighboring cells and local spatial scheduling.

VII. CONCLUSION

In this paper a novel mathematical methodology for performance evaluation on the downlink of cellular networks over fading channels is presented. The proposed approach exploits results from stochastic geometry for the computation of the SINR's MGF, which is shown to be conveniently formulated as a function of a desired-user fading dependent term and the Laplace transform of the interference. By capitalizing on this mathematical formulation, we have been able to obtain exact expressions for the achievable rate and the tangible decoding error probability for various generic fading distribution models including shadowed κ-μ, κ-μ, and η-μ that

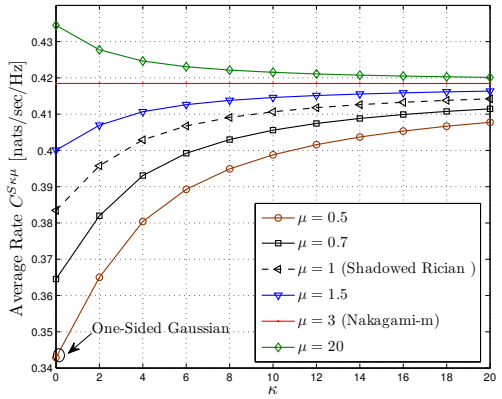

(a) $C^{S\kappa\mu}$ versus κ for $m = m_I = 3$, and $\mu_I = 1$.

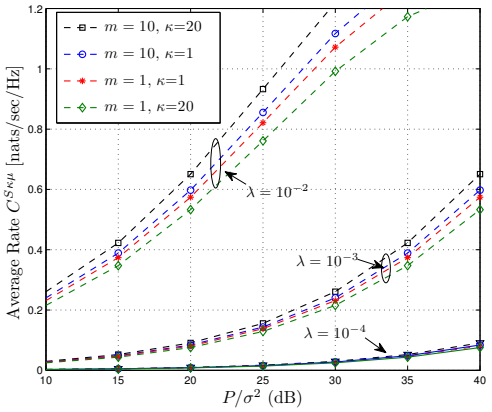

(b) $\mathcal{C}^{S\kappa\mu}$ versus SNR for different values of $\kappa = \kappa_I$ and $m = m_I$ with $\mu = \mu_I = 2$.

Fig. 1. Performance of downlink transmission over shadowed κ-μ fading. Setup: $\Omega_I = \Omega$, $\kappa_I = \kappa$, $\lambda = 10^{-4}$, and $\alpha = 3$.

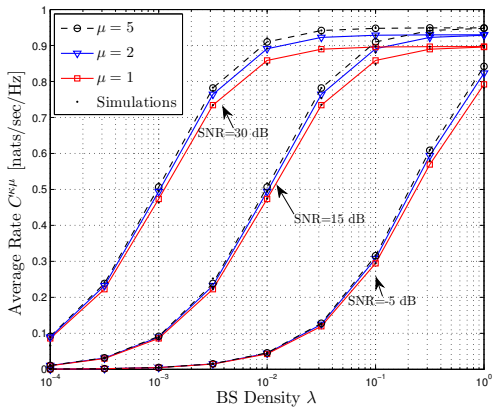

Fig. 2. $C^{\kappa\mu}$ versus BS density λ for different values of $\mu = \mu_I$ with $\kappa = 1.5$. Setup: $\Omega_I = \Omega$, $\kappa_I = \kappa$, $\lambda = 10^{-4}$, and $\alpha = 3$.

account for LOS/NLOS and shadowed fading.

REFERENCES

[1] J. G. Andrews, F. Baccelli, and R. K. Ganti, "A tractable approach to coverage and rate in cellular networks," *IEEE Trans. Commun., vol. 59, no. 11, pp. 3122-3134, Nov. 2011.*

[2] H. Dhillon, R. Ganti, F. Baccelli, and J. Andrews, "Modeling and analysis of K-tier downlink heterogeneous cellular networks," *IEEE J. Sel. Areas Commun.*, vol. 30, no. 3, pp. 550-560, Apr. 2012.

[3] H. ElSawy, E. Hossain, and M. Haenggi, "Stochastic geometry for modeling, analysis, and design of multi-tier and cognitive cellular wireless networks: A survey," *IEEE Commun. Surveys Tuts.*, vol. 15, no. 3, pp. 996-1019, Apr. 2013.

[4] A. Guo and M. Haenggi, "Spatial stochastic models and metrics for the structure of base stations in cellular networks," *IEEE Trans. Wireless Commun.,* vol. 12, no. 11, pp. 5800-5812, Nov. 2013

[5] M. Di. Renzo and P. Guan, "Stochastic geometry modeling of coverage and rate of cellular networks using the Gil-Pelaez inversion theorem." *IEEE Commun. Lett.,* vol. 19, no. 9, pp. 1575-1578, Sep. 2014.

[6] H. ElSawy, A. S-Salem, M.-S. Alouini, and M. Z. Win, "Modeling and analysis of cellular networks using stochastic geometry: A tutorial", *Submitted to IEEE Trans. Information Theory*, Apr. 2016.

[7] M. Di Renzo and W. Lu, "Stochastic geometry modeling and performance evaluation of MIMO cellular networks using the equivalentin-distribution (EiD)-based approach," *IEEE Trans. Commun.*, vol. 63, no. 3, pp. 977-996, Mar. 2015.

[8] L. H. Afify, H. ElSawy, T. Y. Al-Naffouri, and M.-S. Alouini, "The influence of Gaussian signaling approximation on error performance in cellular networks," *IEEE Commun. Lett.,* vol. 19, no. 12, Dec. 2015.

[9] N. Beaulieu and X. Jiandong, "A novel fading model for channels with multiple dominant specular components," *IEEE Wireless Commun. Lett.,* vol. 4, no. 1, pp. 54-57, Feb. 2015.

[10] S. Rangan, T. Rappaport, and E. Erkip, "Millimeter-wave cellular wireless networks: Potentials and challenges," *Proceedings of the IEEE,* vol. 102, no. 3, pp. 366-385, Mar. 2014.

[11] J. F. Paris, "Statistical Characterization of κ-μ Shadowed Fading," *IEEE Trans. Veh. Technol.,* vol.63, no. 2, pp. 518-526, Feb. 2014.

[12] M. D. Yacoub, "The κ-μ distribution and the η-μ distribution," *IEEE Antennas Propag. Mag.,* vol. 49, no. 1, pp. 68-81, Feb. 2007.

[13] S. Parthasarathy and R. K. Ganti, "SIR distribution in downlink Poisson point cellular network with κ-μ shadowed fading," *IEEE Wireless Commun. Lett.,* Vol. 6, no. 1, pp. 10-13, Feb. 2017.

[14] Y. J. Chun, S. L. Cotton, H. S. Dhillon, F. J. Lopez-Martinez, J. F. Paris, and S. Ki Yoo "A Comprehensive Analysis of 5G Heterogeneous Cellular Systems operating over κ-μ Shadowed Fading Channels", *IEEE Trans. Wireless Commun.,* accepted for publication, May 2017.

[15] I. S. Gradshteyn and I. M. Ryzhik, *Table of Integrals, Series and Products,* 5th ed., Academic Publisher, 1994.

[16] M. Di. Renzo, F. Graziosi, and F. Santucci, "A unified framework for performance analysis of CSI-assisted cooperative communications over fading channels," *IEEE Trans. Commun.,* vol. 57, vol. 9, pp. 2552-2557, Sep. 2009

[17] I. Trigui, S. Affes, and B. Liang, "Unified Stochastic Geometry Modeling and Analysis of Cellular Networks in LOS/NLOS and Shadowed Fading" CoRR, vol. arXiv:1609.09389, 2016. [Online].

[18] S. Singh, M. Kulkarni, A. Ghosh, and J. Andrews, "Tractable model for rate in self-backhauled millimeter wave cellular networks," *IEEE J. Sel. Areas Commun.,* vol. PP, no. 99, pp. 1-1, 2015.

[19] Yu. A. Brychkova and N. Saad, "On some formulas for the Appell function $\mathrm{F}_2(a, b, b'; c, c; w; z)$, *Integral Transforms and Special Functions,* vol. 25, no. 2, pp. 111-123, 2014.

[20] K. A. Hamdi, "Capacity of MRC on correlated Rician fading channels," *IEEE Trans. Commun.*, vol. 56, no. 5, pp. 708-711, May. 2008.

[21] M. K. Simon and M.-S. Alouini, *Digital Communication over Fading Channels*. Wiley-Interscience, 2005, vol. 95.

[22] R. Lorenzo, R. Juan, and C. Narcis, "Evaluation of Nakagami fading behaviour based on measurements in urban scenarios," *AEU INT. J. Electron. and Commun.,* vol. 61, no. 2, pp. 135-138, Feb. 2007.